

Interactive and Adaptive Progressive Transmission of Medical Images

Jen-Lung Lo, Saeid Sanei, *Senior Member, IEEE*, and Kianoush Nazarpour, *Student Member, IEEE*

Abstract— An interactive and adaptive joint source-channel coding for progressive transmission of medical images is proposed. This modality is favorable since the region of interest (RoI) is emphasized. The source compression rate is influenced by the proximity to the ROI, which includes significant diagnostic information. Also, the channel coding scalability is affected by both the ROI and the channel characteristics. Therefore both the source compression rate and the parity code length are jointly adapted to (1) the ROI, (2) the channel characteristics, and (3) the required rate or channel capacity. The experimental results verify the effectiveness of the design. The outcome of this project allows transmission of large medical images through narrowband mobile communication channels.

I. INTRODUCTION

Methods based on discrete wavelet transform (DWT) and embedded zerotree wavelet (EZW) [1] have been widely used for progressive transmission of large images [1]-[5]. EZW suits progressive data transmission since it enables hierarchical encoding and decoding. In [6] a framework for solving the end-to-end problem of the progressive transmission of images over noisy channels is presented which allows finding the optimal length of parity codes for each fixed length package for minimum distortion in the decoded images. In [7] a joint source-channel decoder has been introduced. They use a maximum a posteriori (MAP) method to design a joint source-channel coding system. An adaptive source-channel subband coding has been used in [8]. These methods provide a progressive transmission where the receiver reconstructs the transmitted image at various bit rates, using fast and reliable retrieval of RoI for large images. Furthermore, the image sub-blocks are coded separately. Due to the high sensitivity to transmission noise, progressive transmission of images over noisy channels has to be accompanied by an appropriate channel coding or joint source-channel coding scheme [6]. Huffman coding is often used as a variable-length error-free coding technique to further reduce the overall data size [9]. Reed-Solomon (RS) codes are used for channel coding here. The error-correcting capability of RS(p,q) codes is $(p-q)/2$ where p and q are respectively the codeword and the message lengths in terms

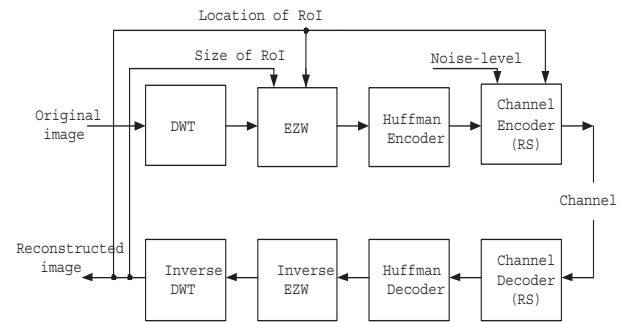


Fig. 1. Overall joint source-channel coding system block diagram

of symbols and are suitable for burst error detection and correction [10].

The proposed method is an interactive and adaptive joint source-channel coding algorithm for which the centre and size of RoI are specified by the user after receiving the low resolution background image. Then, the algorithm adjusts the length of the parity code according to the RoI, and the level of noise automatically. Typically, the ratio of parity code to overall code length is larger for the clinically higher priority areas, i.e. the areas closer to the center of RoI.

The EZW codes the image into streams of six symbols, namely, p , n , z , t , 0, and 1 [11]. The wavelet coefficients $\gamma(x, y)$ are tested against a variable threshold t_n and those above the threshold are coded. The threshold is then halved and the process continues till a certain level of compression is reached. The system block diagram is shown in Fig. 1.

II. VARIABLE SIZE SOURCE CODING

A 3-level Haar wavelet transform (HWT) is used to perform the DWT due to its simplicity and fast implementation. The coefficients in the lowest frequency sub-bands show the background information of the sub-blocks. The coefficients in the higher frequency sub-bands represent the details and edges. The initial threshold is defined as:

$$t_0 = 2^N, \text{ where } N = \log_2 \left\{ \max \left\{ \left| \gamma(x, y) \right| \right\} \right\} \quad (1)$$

The final threshold level determines the size of the bitstream output through the EZW process, the compression ratio of the input images, and the resolution of the reconstructed image. The length of the output bitstream M_i may be expressed in terms of the number of times the threshold is halved as:

This work was supported in part by Cardiff University, Cardiff, UK. The authors are with the Centre of Digital Signal Processing, School of Engineering, Cardiff University, Cardiff CF24 3AA, UK; (e-mails: {LoJ, SaneiS, NazarpourK}@cf.ac.uk).

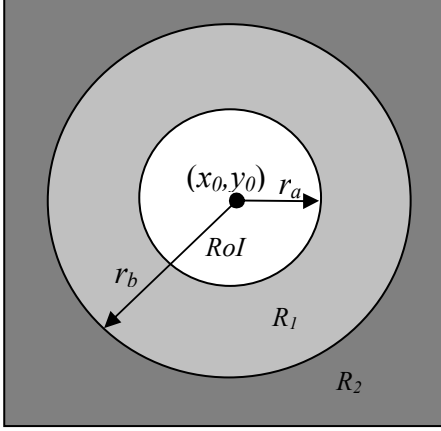


Fig. 2. Areas of different priorities in an image

$$M_i = \sum_{k=1}^{n_i} B(t_{0i} k^{-1}) \quad (2)$$

where $B(t_{0i} k^{-1})$ is the output bitstream of EZW after the initial threshold for i th sub-block t_{0i} halved k times, and n_{Ti} is the total number of times the threshold is halved for the i th sub-block. Fig. 2 shows three regions centered at point (x, y) . The quality of the reconstructed sub-blocks and consequently the compression rate depends on the size of the embedded zerotree. The data in each sub-block is compressed with a different rate depending on the location of the sub-block. The system is designed such that it enables changing the location and size of the RoI without any emphasis on the other regions. In this example, the RoI , R_1 , and R_2 fall respectively within $r \leq r_a$, $r_a < r \leq r_b$, and $r > r_b$. The parameters are shown in Fig. 2, where x and y are the coordinates of the center of RoI assigned by the physician using a mouse click, thereafter both values are sent back to the host. r_a and r_b are the radius of RoI and R_1 , and i and j express the $x-y$ Cartesian coordinate of the ij th sub-block. In the successive stages, the values of r_a and r_b gradually expand to create the reconstructed image of higher quality. In our algorithm, the first transmitted image is the background low resolution image. Then, the reconstruction is progressively continued starting from the RoI .

III. JOINT SOURCE-CHANNEL CODING

The data compressed by EZW, made up of symbols POS, NEG, IZ, ZTR, 0 and 1, can be further compressed using Huffman coding. Consequently, the decoding is performed progressively. But, the progressive bitstream is heavily affected by channel errors [10]. In an RS(p, q) code, $p = 2^m - 1$ is the number of symbols in a codeword and m is the number of bits in each symbol. For each block i

$m_i \sim (M_i, C_i)$, where M_i is the length of the source message, C_i is the length of the parity code. In this adaptive scheme, the reconstruction error is minimized by varying C_i/B_i for i th sub-block, with an overall codeword length

of B_i . Evidently, it is not appropriate to adopt fixed length parity codes in the channel coding to detect and to correct the error data generated over a noisy channel. Since longer messages are more prone to the channel error the parity length should vary accordingly. The image may be divided into n regions (such as in Fig. 2 where $n=3$). The ratio of parity to overall code length for the n regions should follow:

$$C_{RoI}/B_{RoI} > C_{R_1}/B_{R_1} > C_{R_2}/B_{R_2} > \dots > C_{R_{n-1}}/B_{R_{n-1}} \quad (3)$$

Furthermore, the length of parity code is also affected by the noise-level. i.e. $C_{i,j} \sim (r_i, N_j)$, where r_i is the distance from the centre of RoI to the i th sub-block and N_j expresses the j th noise-level. Empirically, the solution to the adaptivity problem can be empirically achieved and approximated using the following two equations:

$$C_{i,j} = (1 - e^{-F_j}) B_i \quad (4)$$

$$F_j = \begin{cases} 0.36 & r_i > r_b \\ 0.25 + 0.12 N_j & r_a < r_i \leq r_b \\ 0.24 + 0.14 N_j & r_i \leq r_a \end{cases} \quad (5)$$

Therefore, the optimization problem for measuring the bit number in each symbol, m_i , can be expressed as (the index j has been discarded for simplicity):

$$\hat{m}_i = \arg \min_m \left((2^m - 1) - C_i \right) \quad s. t. \quad (2^m - 1) - C_i > M_i \quad (6)$$

Fig. 3 represents this approximation for different noise-levels (four in this example), for $N_1 = 1, N_2 = 2, N_3 = 3$, and $N_4 = 4$. According to Fig. 3, the percentage of parity codes in a codeword is variable based on the location of the sub-block and the noise-level; for noise-level N_4 a longer parity is required. In the receiver, the RS decoder detects and corrects the error bits. Practically, the system may request for retransmission of the data, but in the proposed system, a '0' is assigned to the transmitted sub-block in the case of any bit in error. The performance of the system is evaluated for different noise-level using peak signal-to-noise ratio (PSNR) defined as $PSNR(dB) = 10 \log_{10} S^2 (MSE/mlk)^{-1}$, where S is the maximum image amplitude, and l and k are the image dimensions. For the case of monochrome images, $m=1$, while for color images $m=3$. Besides, $MSE = \|\hat{I} - I\|_2^2 / \|\hat{I}\|_2^2$ where \hat{I} and $\|\cdot\|_2^2$ represent the reconstructed image I , and the squared Euclidean norm, respectively.

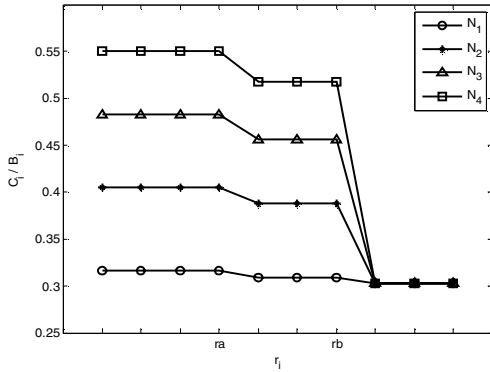


Fig. 3. The ratios between the lengths of parity code and overall codeword in different regions at various noise-levels, N_1, N_2, N_3 and N_4 according to equation (4).

IV. SIMULATION RESULTS

The developed algorithm has been tested on two different images. One a 150×123 color dental implant image and another one a 508×512 pixel monochrome x-ray bone image transmitted via TCP/IP as in Fig. 1. The error bits are generated by randomly inverting a certain percentage of bits in the EZW bitstream. To verify the effectiveness of the system the image regions are progressively transmitted in four stages of P_1, P_2, P_3 and P_4 . During P_1 the background image is transmitted. P_2 and P_3 are the second and third stages, both for transmission of RoI , R_1 , and R_2 . P_4 is mainly to transmit the details of RoI . The transmission can continue to achieve the desired compression rate in a final stage. Table I shows the compression ratios at these stages, with the parity codes under different noise levels, N_1, N_2, N_3 , and N_4 indicating different channel situations. Here, it is assumed that this information is known to the system and therefore the parity length is automatically adjusted to that. In Fig. 4, the input image is transmitted under the N_4 noise-level. As in Fig. 5, the PSNR decreases monotonically for all the regions, with higher values for the regions of higher priorities. This verifies the adaptivity of the variable parity length scheme to the changes in both the region content and the channel noise level. Fig. 6(a) shows the background image sent during P_1 stage. Fig. 6(b) is progressively reconstructed image after stage P_2 in which the RoI, R_1 , and R_2 are reconstructed. At this stage, the center of RoI is denoted by the user via mouse click. Fig. 6(c) represents the reconstructed image at stage P_3 during which the regions ROI, R_1 and R_2 are reconstructed. The resolution of the regions of RoI and R_1 are gradually increased. Fig. 6(d) is the final and complete image after stage P_4 . The system has been modified to allow variable lengths for both message and parity. It is clear, then, from Fig. 7 that the error sub-blocks in the RoI and its vicinity have been effectively

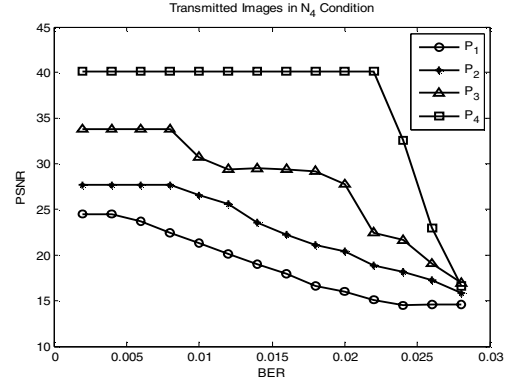


Fig. 4. PSNR at different stages of transmission P_1, P_2, P_3 , and P_4 , versus BERs under N_4 noise-level condition.

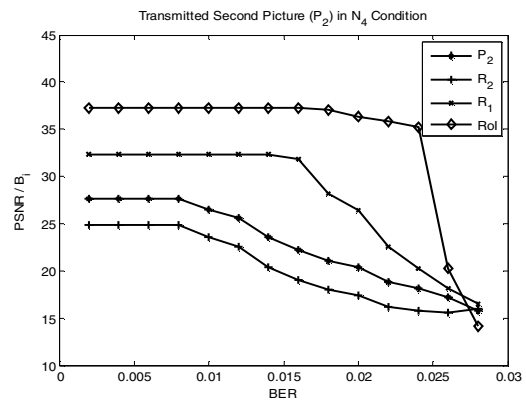


Fig. 5. PSNR for reconstruction of RoI, R_1 and R_2 in the P_2 image regions at different BERs under N_4 noise-level condition.

TABLE I
OVERALL IMAGES COMPRESSION RATIOS AT DIFFERENT CHANNEL NOISE LEVELS.

Ratios	P_1	P_2	P_3	P_4
N_1	8.311	2.440	1.358	0.962
N_2	8.311	2.213	1.197	0.840
N_3	8.311	2.036	1.082	0.755
N_4	8.311	1.862	0.968	0.670

mitigated and the overall system has been improved. A set of similar results is illustrated for a monochrome x-ray image in Fig. 8.

V. CONCLUSIONS

A new adaptive source-channel coding for the progressive transmission of medical images has been proposed. The system is adaptive to both image content and channel specifications. The capability of data error detection and correction and image transmission time and efficiency are the key roles in the process. The presented results verify the effectiveness of the system in terms of both adaptivity and flexibility of interaction. A MATLAB-based TCP/IP connection has been established to demonstrate the proposed interactive and adaptive progressive transmission system.

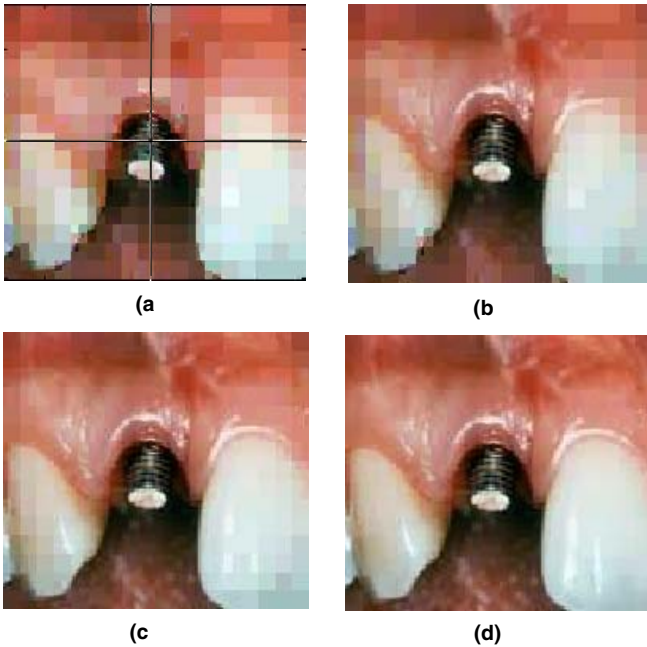


Fig. 6. The error-free transmitted implant image over the low-noise channel (a) the background image at stage P_1 and the location of RoI in the centre of the image, (b) the transmitted image after stage P_2 , (c) the transmitted image after stage P_3 , and (d) shows the completely decoded image after stage P_4 .

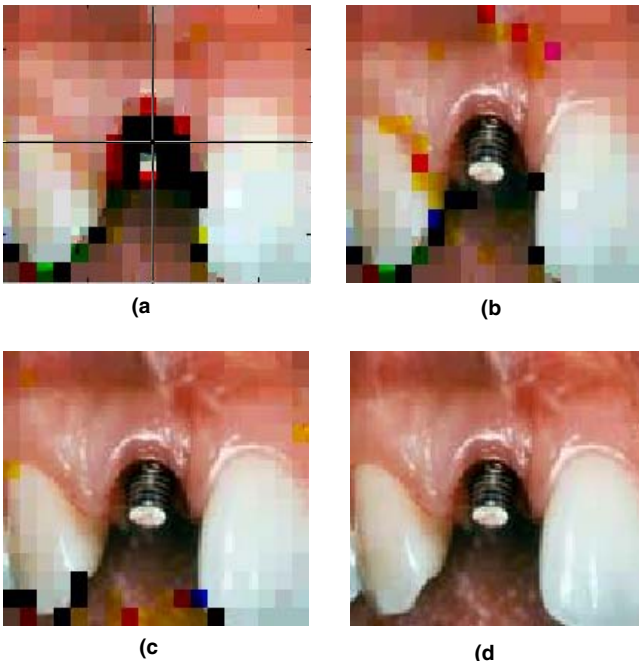


Fig. 7. The decoded implant image with variable length of parity codes over the noisy channel: (a) the background image and the location of RoI selected in the centre of image reconstructed after stage P_1 , (b) the reconstructed image after stage P_2 , some error sub-blocks are found in the vicinity of RoI , (c) the reconstructed image after stage P_3 ; the error sub-blocks are still found in the vicinity of the RoI but not inside the RoI , and (d) the complete transmitted image having no sub-blocks in error.

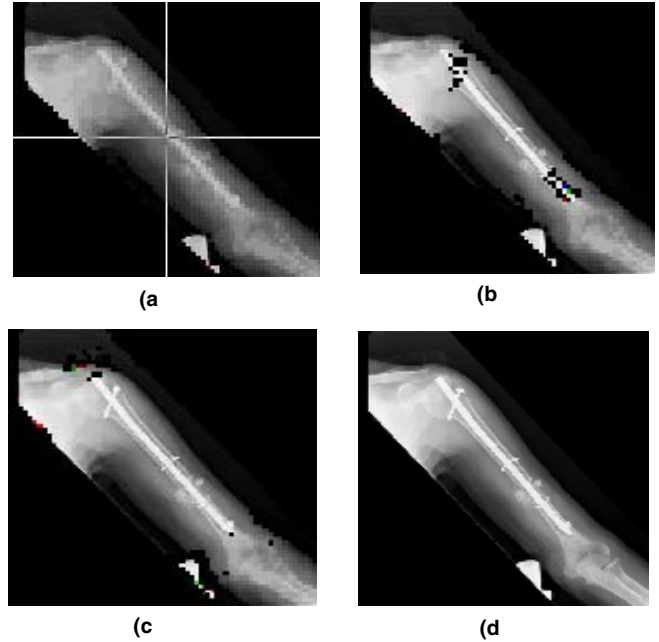


Fig. 8. The decoded x-ray bone image decoded in the same procedure as of Fig. 7.

REFERENCES

- [1] J. M. Shapiro. "Embedded image coding using zerotree of wavelet coefficients," *IEEE Trans. Sig. Process.*, vol. 41, no. 12, pp. 3445-3462, 1993.
- [2] F. Etemadi, and H. Jafarkhani, "An Efficient Progressive Bitstream Transmission System for Hybrid Channels With Memory," *IEEE Trans. Multimedia Sig. Proc.*, vol. 8, no. 6, pp. 1291-1298, 2006.
- [3] V. M. Stankovic, R. Hamzaoui, Y. Charfi, and X. Zixiang, "Real-time unequal error protection algorithms for progressive image transmission." *IEEE J. Sel. Areas Commun.*, vol. 21, no. 10, pp. 1526 - 1535, 2006.
- [4] W. Song, C. Kim and S. Lee, "Progressive compression and transmission of PointTexture images," *J. Visual Comm. Image Rep.*, vol. 17, no. 5, pp. 1090-1107, 2006.
- [5] C. Shang-Kuan and L. Ja-Chen, "Fault-tolerant and progressive transmission of images," *Pattern Recognition*, vol. 38, no. 12, pp. 2466-2471, 2005.
- [6] H. Yousefi'zadeh, H. Jafarkhani, and F. Etemadi, "Distortion-optimal transmission of progressive images over channels with random bit errors and packet erasures," in *Proc. DCC'04*, pp. 132-141, 2004.
- [7] J. Chebil, B. Boashash, and M. Deriche, "Combined source channel decoding for image transmission over fading channels," in *Proc. 9th APCC 2003*, vol. 1, pp. 297-301, 2003.
- [8] M. Srinivasan and R. Chellappa, "Joint source-channel subband coding of images," in *Proc. ICASSP97*, vol. 4, 21-24, pp. 2925-2928, 1997.
- [9] R. G. Gallager, "Variations on a theme by Huffman," *IEEE Trans. Info. Theory*, vol. 24, no. 6, pp. 668-674, 1978.
- [10] J. Chen and P. Owsley, "A burst-error correcting algorithm for Reed-Solomon codes," *IEEE Trans. Info. Theory*, vol. 38, no. 6, pp. 1807-1812, 1992.
- [11] Clemens Valens, "EZW Encoding," at <http://perso.wanadoo.fr/polyvalens/clemens/ezw/ezw.html>